JPR Advance Access published March 9, 2015

Journal of
Plankton Research

plankt.oxfordjournals.org

J. Plankton Res. (2015) 37(2): 1–17. doi:10.1093/plankt/fbv011

Grazer and viral impacts on microbial growth and mortality in the southern California Current Ecosystem

ALEXIS L. PASULKA[1]*, TY J. SAMO[2] AND MICHAEL R. LANDRY[1]

[1]SCRIPPS INSTITUTION OF OCEANOGRAPHY, UCSD, 9500 GILMAN DRIVE, LA JOLLA, CA 92037, USA AND [2]DEPARTMENT OF OCEANOGRAPHY, UNIVERSITY OF HAWAI'I AT MANOA, 1000 POPE RD, HONOLULU, HI 96822, USA

*CORRESPONDING AUTHOR: apasulka@caltech.edu

Received November 25, 2014; accepted February 11, 2015

Corresponding editor: John Dolan

Protistan grazers and viruses are major agents of mortality in marine microbial communities with substantially different implications for food-web dynamics, carbon cycling and diversity maintenance. While grazers and viruses are typically studied independently, their impacts on microbial communities may be complicated by direct and indirect interactions of their mortality effects. Using a modification of the seawater dilution approach, we quantified growth and mortality rates for total phytoplankton and picophytoplankton populations (*Prochlorococcus*, *Synechococcus*, picoeukaryotes) at four contrasting sites in the California Current Ecosystem. Grazing mortality was significant in 10 of 15 cases, while viral effects were significant for 2 cases. Nonetheless, mortality estimates for the entire phytoplankton community based on chlorophyll *a* were 38 ± 13% higher when viral effects were included, relative to grazing alone. Mortality estimates for picophytoplankton varied in space and among groups. We also explored a potential methodological constraint of this method and hypothesize that heterotrophic bacteria may be affected by the dilution of their growth-sustaining substrates. For all picophytoplankton, estimates of grazing and viral mortality were inversely related within and across experiments. Indirect interactions among grazers and viruses may be important to consider if there are tradeoffs in the grazing and virus resistance strategies of prey/host cells.

KEYWORDS: microzooplankton grazing; viral lysis; picophytoplankton; mortality

INTRODUCTION

Mortality processes within microbial communities play key roles in regulating biomass, species composition and elemental cycling (Pomeroy *et al.*, 2007; Suttle, 2007). Protistan grazers, the primary consumers of phytoplankton and bacteria (Sherr and Sherr, 1994, 2000), account,

available online at www.plankt.oxfordjournals.org

on average, for the direct utilization of more than two-thirds of ocean primary production (Calbet and Landry, 2004). Viral lysis of microbial hosts cycles 6–26% of photosynthetic production (Wilhelm and Suttle, 1999) and can be the dominant loss process under many ecological circumstances (Proctor and Fuhrman, 1990; Suttle, 1994; Weinbauer and Peduzzi, 1995; Brussaard, 2004). As mortality agents, grazers and virus have substantially different effects on carbon and energy flows, which may vary appreciably within and among systems depending on the relative strengths of these loss processes. Viruses shunt most of the carbon from their hosts to dissolved organics and, eventually, carbon dioxide (CO_2) due to bacterial respiration (Fuhrman, 1999; Suttle, 2005), while protistan grazers are more important as a trophic transfer link to higher consumers (Sherr and Sherr, 1988; Landry and Calbet, 2004). Grazers and viruses also differ inherently in their expected impacts on microbial diversity, with viral mortality more likely to be defined by host-specificity and population-selective impact (Thingstad, 1998, 2000; Brussaard, 2004; Weinbauer, 2004) relative to the broader size- or total biomass-based impact of grazing (Gonzalez *et al.*, 1990; Sherr *et al.*, 1992; Hansen *et al.*, 1997). Such differences underlie recent interest in comparing and contrasting the magnitudes of grazer and virus mortality effects on microbial populations in a variety of marine systems (Baudoux *et al.*, 2007, 2008; Taira *et al.*, 2009; Evans and Brussaard, 2012; Tsai *et al.*, 2013a, b).

Previous studies in the southern California Current Ecosystem (CCE) have demonstrated that experimentally determined process rates, as measured by the standard dilution method for phytoplankton growth and microzooplankton grazing and gut fluorescence for mesozooplankton grazing, explain a large portion of the variability (91%) in net growth rates of ambient phytoplankton biomass (chlorophyll *a*) observed over 3–5 day periods following drogued-drifters (Landry *et al.*, 2009). Such results imply that other processes, such as direct cell sinking, only contributed in minor ways to phytoplankton dynamics in the water parcels examined. However, true phytoplankton growth rates and loss processes may have been underestimated in these experiments because viral impacts were not measured.

One goal of the present study was to reconsider these rate relationships by assessing the magnitudes of viral lysis and protistan grazing on phytoplankton vital rates over a range of late summer conditions in the southern CCE region. We used the Evans *et al.* (Evans *et al.*, 2003) modification of the seawater dilution approach to determine the rates simultaneously within the same experimental design. We measured chlorophyll *a* to determine the mean rates for the whole community and also quantified picophytoplankton (*Prochlorococcus*, *Synechococcus* and picoeukaryotes) using flow cytometry, to evaluate mortality patterns among different populations.

An additional goal of this study was to explore the potential impacts of manipulating microbial communities (i.e. applying the modified dilution method) across a range of environmental conditions. Although the dilution approach has been applied in field studies (Kimmance and Brussaard, 2010), the efficacy of the method depends on many assumptions that have not been explored as extensively as the dilution grazing rate estimates. While some of the limitations of the modified dilution method have been considered previously (e.g. consequences of cells being infected prior to dilution, length of lytic cycles and density-dependent predator/prey dynamics; Jacquet *et al.*, 2005; Kimmance *et al.*, 2007), the notion that heterotrophic bacteria may violate dilution method assumptions has not. This is particularly relevant for applying this approach in natural systems to compare and contrast rates across a range of environmental conditions.

One of the main assumptions of the dilution method is that prey growth rate is independent of dilution (Landry and Hassett, 1982). While nutrient amendments are an effective way to ensure that phytoplankton growth rates are independent of the dilution effect (Landry *et al.*, 1995), heterotrophic bacteria may still be affected by the dilution of growth-limiting organic substrates (Amon and Benner, 1996), which are far more difficult to compensate for. Furthermore, even in the absence of nutrient amendments, the different filtration cutoffs between the two dilution series (e.g. 0.1 μm versus 30 kDa) may alter the suite of dissolved organic matter (DOM) available to heterotrophic bacteria relative to concentrations of nutrients (Amon and Benner, 1996). Heterotrophic bacterial dynamics are important to consider because of their direct (Malfatti and Azam, 2009) and indirect (Weinbauer *et al.*, 2011; Shelford *et al.*, 2012) interactions with other components of the microbial community. Since heterotrophic bacterial communities vary greatly in abundance, biomass, composition and production in the CCE (Fuhrman and Azam, 1980; Allen *et al.*, 2012; Samo *et al.*, 2012), the effects of manipulation on these interactions could vary substantially under different environmental conditions.

Our results reveal complexity in grazer selectivity, variable responses of heterotrophic bacteria to dilution and inverse relationships between virus and grazer impacts. Indirect interactions between grazers and viruses may be substantial in marine microbial communities and difficult to resolve as purely mortality effects in dilution-based experiments. Here, we attempt to explore both ecological and methodological interpretations of modified dilution results, highlighting areas of research that need further study.

METHOD

Experimental site and sampling

Dilution experiments were carried out in the southern CCE during a research cruise in October 2008 (Fig. 1). The California Current System (CCS) resides in the eastern portion of the anticyclonic North Pacific Subtropical Gyre (Lynn and Simpson, 1987), where strong equatorward winds in the spring and summer months drive coastal upwelling (Hickey, 1979; Checkley and Barth, 2009). This coastal upwelling delivers new nutrients to the ecosystem, resulting in a seasonal increase in primary production (Checkley and Barth, 2009). As nutrient-rich upwelled water moves offshore, thermal fronts at the interface with warmer oligotrophic offshore waters (Mann and Lazier, 2006) typically separate systems of strikingly different pelagic communities and biological productivity (Brink and Cowles, 1991; Strub and James, 2000; Checkley and Barth, 2009). Mesoscale variability within this region makes it ideal for studying the dynamics of lower trophic levels under varying environmental conditions. In the present study, we conducted experiments within the mixed layer at four locations varying in surface chlorophyll *a*, distance from shore and from contrasting adjacent water masses at a thermal front (Fig. 1).

Modified dilution method

In order to quantify the contributions of grazers and viruses to picophytoplankton mortality in the same experimental design, we employed the modified dilution method (Evans *et al.*, 2003; Kimmance and Brussaard, 2010), which uses sequential dilution of the natural community with two different types of filtered seawater to reduce predator–prey and viral–host encounter rates. We set up four experiments using mixed-layer seawater collected with Niskin bottles attached to a CTD Rosette (depth of collection = 15, 20, 8 and 20 m for Experiments 1, 2, 3 and 4, respectively). To assess grazing mortality, diluent water was filtered through a 0.1 μm Acropak filter capsule directly from the Niskin bottles into 2.2 L incubation bottles for final dilution levels of ~20, 40, 60, 80 and 100% of whole seawater. We used 0.1 μm filter capsules in order to be consistent with previous dilution experiments performed in this region (Landry *et al.*, 2009). The potential consequences of 0.1 μm filtration on the viral populations are discussed in the Results section. To measure viral mortality, a parallel dilution series was set up with 30 kDa filtered water (Baudoux *et al.*, 2007). A 10 L carboy was filled with 0.1 μm filtered seawater directly from the Niskin, and subsequently run through a 30 kDa tangential-flow filtration system (EMD Millipore). The 30 kDa filtrate was added to 1 L incubation bottles for final dilution levels of ~45, 70 and 100% of whole seawater. Levene's test (Zar, 1999) was used to confirm that different sample sizes across the dilution series did not violate the assumption of homogeneity of variances. For both dilution series, whole seawater (i.e. unfiltered seawater) was gently added to each incubation bottle following the addition of the pre-measured volumes of filtrate, and all treatments were done in duplicate. Nitrate (1 μM) and phosphate (0.06 μM) were added to incubation bottles (Landry *et al.*, 1995). One set of 100% whole seawater replicates was kept as non-

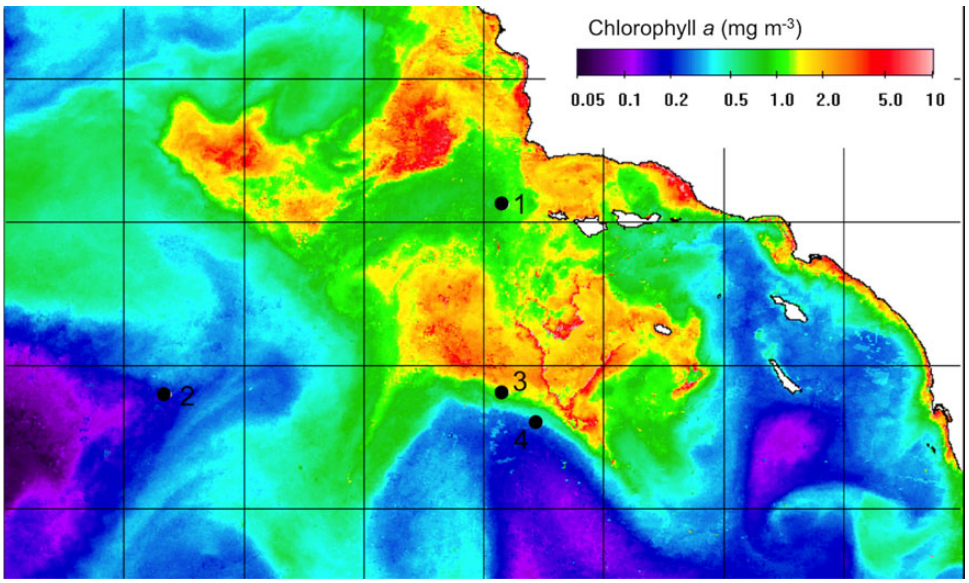

Fig. 1. Satellite image of near-surface chlorophyll *a* (mg Chl *a* m^{-3}) in the southern CCE. Chlorophyll *a* is merged from MERIS, MODIS-Aqua, MODIS-Terra and SeaWiFS data for 16–20 October. Solid-black circles indicate the location and number of each experiment.

nutrient controls to estimate *in situ* growth rates in each experiment. Experimental bottles were incubated in flow-through incubators on deck at *in situ* light (30% of incident PAR, approximately the mixed-layer depth of collection) and mixed-layer temperature conditions. Although different bottle sizes were used for the grazing and viral dilution series, population changes in the whole sea water bottles (100%) over 24 h were the same in the 1 and 2.2 L bottles. We therefore saw no evidence that bottle size influenced the experimental results.

Initial and final samples for flow cytometry and microscopy were taken to quantify the growth rates of the microbial community. To calculate growth and mortality in each dilution series, the following equations from Evans *et al.* (Evans *et al.*, 2003) were used.

$$k = (\mu - m_v) - m_g \times D \quad (0.1\ \mu\text{m series}) \qquad (1)$$

$$k = m - (m_v + m_g) \times D \quad (30\ \text{kDa series}) \qquad (2)$$

where k is the measured net growth rate (day^{-1}), μ the instantaneous growth rate of the phytoplankton, m_v the mortality due to viruses, m_g the mortality due to grazing and D the dilution level (determined by bottle volumes). As in Evans *et al.* (Evans *et al.*, 2003), the mortality of phytoplankton due to viral lysis was quantified by subtracting the measured mortality in the traditional dilution series (m_g) [equation (1)] from the mortality in the viral dilution series ($m_g + m_v$) [equation (2)]. The instantaneous growth (μ) rate determined from the dilution experiment was corrected to an *in situ* rate (μ_{env}) by addition or subtraction of the difference between the average apparent growth rate (k) in the undiluted (i.e. 100% seawater) incubation bottles without added nutrients and the undiluted incubation bottles with added nutrients. In waters where nutrient limitation may be a problem, adding nutrients can reduce the influence of dilution on picophytoplankton growth. However, with nutrient additions, the y-intercept of the dilution regression may not reflect the actual picophytoplankton growth rate. Therefore, the true growth rate is estimated from the observed net rates in the undiluted samples with and without nutrient amendments, assuming similar grazing (Andersen *et al.*, 1991; Landry *et al.*, 1995). Analysis of covariance, which blends analysis of variance and regression, was used to determine the significance of the mortality rates calculated using equations (1) and (2). Using MATLAB (The MathWorks, Inc.), we determined the significance (P) of the slope (m_g and $m_g + m_v$) and intercept (μ) for each regression individually (i.e. slopes significantly different from zero) as well as the significance between the slopes of the regression lines (i.e. significance of m_v). A significance level of $\alpha = 0.05$ was used for the statistical analyses. In the cases where significant differences between m_g and m_{g+v} were not detected, a power analysis was done to test the sensitivity of the modified dilution approach to detect viral mortality (Kimmance *et al.*, 2007) and determine if non-significant rates are a result of actual low viral mortality or methodological limitations.

Flow cytometric analyses

For population-specific rate determinations, we enumerated populations of *Prochlorococcus* spp. (PRO), *Synechococcus* spp. (SYN), picoeukaryotes (PEUK) and heterotrophic bacteria using flow cytometry. Initial and final samples (1 mL) were collected from each bottle. They were preserved with 0.5% paraformaldehyde, flash frozen in liquid nitrogen and stored at −80°C for <1 year. Thawed samples were stained with Hoechst 34442 (1 μg mL^{-1}) (Monger and Landry, 1993) and analyzed with a Beckman–Coulter Altra Flow Cytometer equipped with two argon ion lasers, tuned to UV (200 mW) and 488 nm (1 W) excitation at the SOEST Flow Cytometry Facility, University of Hawaii. Scatter (side and forward) and fluorescence signals were collected using appropriate filters for Hoechst-bound DNA, phycoerythrin and chlorophyll. Fluorescence signals were normalized to 0.5 and 1.0 μm yellow–green polystyrene beads (Polysciences Inc., Warrington, PA, USA). Population designations were determined using FlowJo (Tree Star, Inc.) based on the scatter and fluorescence signals.

Virus enumeration

Viruses were enumerated by epifluorescence microscopy (Nobel and Fuhrman, 1998; Patel *et al.*, 2007). The samples (1 mL) were gently filtered (<0.5 mmHg) onto 0.02 μm Anodisc filters with HA backing filters, dried and stained for 15 min with SYBR Gold (0.25% final concentration). After staining, the filters were dried in the dark and mounted onto slides with 0.1% *p*-phenylenediamine anti-fade mounting solution.

Immediately after the slides were prepared, viruses were counted at 1000× using an Olympus BX51 epifluorescence microscope with a 100× objective and long-pass FITC-filter. A 10 × 10 eyepiece micrometer (98.8 × 98.8 μm) was used to designate counting areas. To minimize particle fading, a few but consistent number of squares were counted on each slide field, enumerating at least 200 viruses on each filter. Viral concentration was calculated based on the Anodisc internal diameter.

Protistan community biomass and composition

Initial concentrations of protists in each experiment were determined using epifluorescence microscopy as described

by Taylor *et al.* (Taylor *et al.*, 2012). Seawater samples (500 mL) were fixed and stained according to a modified protocol of Sherr and Sherr (Sherr and Sherr, 1993), which involves the sequential addition of 260 μL of alkaline Lugol's solution, 10 mL of buffered formalin and 500 μL of sodium thiosulfate. Preserved samples were stained with 1 mL of proflavin (0.33% w/v) in the dark for 1 h, and 1 mL of DAPI (0.01 mg mL^{-1}) just prior to filtration. Samples were filtered onto black polycarbonate filters, mounted on glass slides with immersion oil and kept frozen at −80°C for <1 year. The slides were digitally imaged using a Zeiss Axiovert 200 M inverted epifluorescent compound microscope. A minimum of 20 random positions were imaged for each slide. Each position image consisted of four different color channels (chlorophyll *a*, DAPI, FITC and phycoerythrin), and these separate channel images were composited into 24-bit RGB images prior to analysis.

Images were analyzed using ImagePro software. Each cell was manually identified and grouped into four plankton groups: diatoms, prymnesiophytes, flagellates and dinoflagellates. Photosynthetic protists (autotrophs + mixotrophs) were distinguished from heterotrophic protists by the presence of chlorophyll, seen as red autofluorescence under blue light excitation (Sherr and Sherr, 1993). Cells were grouped into three size categories (Pico, <2 μm; Nano, 2–20 μm; Micro, 20–200 μm) based on the length of their longest axis. Length (*L*) and width (*W*) measurements were converted to biovolumes (BV; μm^3) by applying the geometric formula of a prolate sphere ($BV = 0.524LWH$). For the unmeasured dimension of cell height (*H*), we used $H = W$. Carbon (C; pg $cell^{-1}$) biomass was computed from BV using the equations of Menden-Deuer and Lessard (Menden-Deuer and Lessard, 2000): $C = 0.216BV^{0.939}$ for non-diatoms, and $C = 0.288BV^{0.811}$ for diatoms.

To account for ciliates, which are poorly preserved using the protocol above, 100 mL of seawater was preserved at sea with acid Lugol's (5% final concentration) and stored at room temperature until further analysis. In the lab, the samples were fixed with formalin (2% final concentration), filtered onto polycarbonate filters, counted on glass slides and then imaged using a Zeiss Axiovert 200 M inverted microscope at 200× magnification (Freibott *et al.*, 2014). The length, width and characteristic shape of each ciliate was used to calculate cell biovolume, which was converted to carbon biomass using the Putt and Stoecker (Putt and Stoecker, 1989) conversion of $C = 0.19 \times BV$ for aloricate oligotrichs. Microbial eukaryote abundance and composition were determined for the cast prior to that used for the dilution experiments. However, because we followed a Lagrangian drifter (Landry *et al.*, 2009), we were able to repeatedly sample the same water mass.

Chlorophyll, nutrients and dissolved organics

Samples for chlorophyll *a*, nutrients (nitrate and phosphate) and dissolved organics were taken from Niskin bottles at the start of each experiment. Samples for chlorophyll *a* were also taken from experimental bottles after 24 h. Chlorophyll *a* samples (256 mL) were filtered onto GF/F filters. Pigments were extracted in 90% acetone at −20°C in the dark for 24 h prior to analysis on a Turner Design Model 10-AU fluorometer. Measurements were made before and after the addition of 10% HCl to determine both chlorophyll *a* and phaeopigment concentrations (Strickland and Parsons, 1972). Initial chlorophyll concentrations used to calculate *k* (the measured net growth rate; day^{-1}), were estimated from the dilution factor (as determined by initial SYN concentration in each bottle).

Samples for the analysis of nitrate and phosphate were collected from Niskin bottles into 45 mL plastic test tubes and stored frozen at −80°C until analysis ashore within 2 months of collection. Nutrients were analyzed by flow injection at the nutrient laboratory of the University of California, Santa Barbara on a Lachat Instruments QuikChem-8000 using standard wet-chemistry methods (Gordon *et al.*, 1993).

For total organic carbon (TOC), unfiltered seawater samples (40 mL) were acidified with hydrochloric acid to pH ~2 and analyzed on a Shimadzu 500 V-CSN/TNM-1 TOC analyzer. For particular organic carbon (POC) and particular organic nitrogen (PON), 2 L of seawater was filtered onto 25 mm pre-combusted (450°C, 6 h) Whatman GF/F filters. The filters were exposed to concentrated HCl vapor to remove inorganic carbon, and C and N values were determined at the Scripps Institution of Oceanography Analytical Facility using a Costech Elemental Analyzer according to standard protocols. Although we report both TOC and POC, we did not compute dissolved organic carbon (DOC) as the difference between these two values because POC and TOC measurements were done on very different sample volumes (100 μL injection versus 2 L filtration). DOC was generally higher by an order of magnitude, and TOC is assumed to be mostly composed of DOC. Details of TOC, POC and PON analyses are in Samo *et al.* (Samo *et al.*, 2012).

RESULTS

Environmental conditions and microbial community patterns

Our four experiments varied in terms of environmental characteristics (Table I) and community structure (Table II). Experiment 1 captured an intrusion of warmer offshore

Table I: Environmental characteristics of experimental sites in the CCE

Exp	Lat	Lon	Depth (m)	T (°C)	Chl (μg L^{-1})	TOC (μM C)	PON (μM)	POC (μM)	Phosphate (μM)	Nitrate (μM)
1	34.11	−120.84	12	17.3	0.31	59.20	0.7	5.0	0.31	0.42
2	32.80	−123.66	20	17.6	0.18	66.88	0.4	3.3	0.32	0.41
3	32.82	−120.84	8	14.8	1.84	64.98	2.9	15.6	0.38	1.90
4	32.60	−120.56	20	17.2	0.21	61.30	0.6	4.1	0.33	0.12

Data are from water collected with Niskin bottles attached to a CTD Rosette in the morning (~2 a.m.) before the start of each experiment (~6 p.m.). For Experiment 1, the water for environmental analysis was collected from 12 m and the water for the experiments was collected from 15 m, but both depths were within the mixed layer.

Table II: Abundance (± standard deviation) of microbial community components at the start of each experiment

Exp	Auto Euk (10^5 mL^{-1})	Hetero Euk (10^5 mL^{-1})	Viruses (10^7 mL^{-1})	Hbact (10^5 mL^{-1})	PRO (10^4 mL^{-1})	SYN (10^4 mL^{-1})	PEUK (10^3 mL^{-1})
1	22.1	9.1	2.0 ± 0.1	10.2 ± 1.1	3.2 ± 0.1	5.4 ± 0.2	9.9 ± 0.5
2	24.7	14.8	1.2 ± 0.1	4.4 ± 0.1	2.4 ± 0.1	0.4 ± 0.0	3.7 ± 0.7
3	41.9	19.1	1.6 ± 0.3	5.0 ± 0.3	ND	0.4 ± 0.0	5.7 ± 0.8
4	18.1	4.5	2.2 ± 0.3	7.1 ± 1.3	7.7 ± 0.5	1.6 ± 0.1	7.8 ± 0.5

For viruses, Hbact (heterotrophic bacteria), PRO, SYN and PEUK, the data are an average of the undiluted (100% seawater) replicates at the start of the experiment. Microbial eukaryote abundance (Auto Euk and Hetero Euk) was from the CTD cast prior to the cast used for experiment set up.
ND, no detection.

waters that had come close to the coast (Fig. 1). Experiment 2 was conducted furthest offshore in warm, oligotrophic waters. Experiments 3 and 4 were positioned on either side of an east–west-oriented thermal front (Fig. 1) (Landry *et al.*, 2012). Experiment 3 was on the cold side of this deep-ocean front in waters of coastal origin that had advected south and westward from the Pt. Conception upwelling center. Experiment 4 was located on the warm side of the front in waters of subtropical origin. While environmental conditions during Experiment 1 had slightly higher concentrations of chlorophyll *a* and POC relative to Experiments 2 and 4, the waters for Experiment 3 were notably higher in chlorophyll *a*, nitrate, POC and PON (Table I; see Landry *et al.*, 2012, for more details on the frontal feature).

SYN and PEUK exhibited similar abundance patterns, with the highest concentrations inshore for Experiment 1, whereas PRO was most abundant on the warm side of the front in Experiment 4 (Table II). All picophytoplankton had low abundances offshore in the waters sampled for Experiment 2, but PRO was entirely absent in Experiment 3 (the colder, richer side of the front). Photosynthetic protists were notably more abundant in the cold, nitrate-rich waters sampled for Experiment 3. Heterotrophic bacterial abundance was highest inshore for Experiment 1 and lowest offshore in Experiment 2.

Grazers and viruses showed opposite abundance trends, with viruses more numerous in Experiments 1 and 4 and grazers more abundant in Experiments 2 and 3. When converted to carbon biomass, however, grazers were about twice as high in experiments conducted with waters of coastal origin (~13 μg C L^{-1}, Experiments 1 and 3, Fig. 2) compared with waters of offshore origin (~6 μg C L^{-1}, Experiments 2 and 4, Fig. 2). The protistan assemblages were similar in Experiments 2 and 4, consisting mainly of nano-sized flagellates and dinoflagellates. Ciliates contributed a greater proportion of protistan biomass in Experiments 1 and 3. However, nano-sized grazers dominated the biomass in Experiment 3, whereas nano-sized and micro-sized protists contributed more equally to grazer community biomass in Experiment 1.

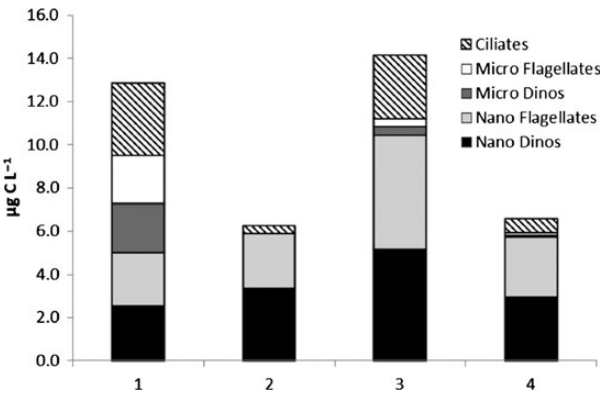

Fig. 2. Composition and carbon biomass (μg C L^{-1}) of the heterotrophic protistan community at the start of each dilution experiment (*x*-axis).

Growth and mortality rate

Rates and statistics for all experiments are presented in Table III. Examples of the plotted results are shown in Fig. 3 for Experiment 3. A small gradient of viral concentration is evident in the 0.1 μm dilution series (Fig. 3 and Supplementary data, Fig. S1). Since algal viruses range from 20 to 200 nm (Brussaard, 2004), viruses of larger algal cells may have been retained on the 0.1 μm filter. However, smaller viruses associated with the smaller host cells in this study (SYN, PRO and PEUKs) were most likely not affected.

Sensitivity tests revealed that statistical power was, in most cases, able to detect differences as low as 10% in mortality slopes (e.g. a viral mortality ~0.1 day^{-1}). In two cases (SYN and Chl *a* in Experiment 4), we were not able to detect viral mortality <0.2 day^{-1}, and in one case (PRO Experiment 2), the statistics were not able to detect viral mortality as high as 0.3 day^{-1}. These are in the range of values reported for this method by Kimmance *et al.* (Kimmance *et al.*, 2007).

Table III: Growth and mortality rates (day^{-1}) from each experiment for total phytoplankton (chlorophyll a) and for picoplankton populations of SYN, PRO, PEUK

	Exp. 1	Exp. 2	Exp. 3	Exp. 4
Chl *a*				
μ_{env}	0.46	0.35	0.79	0.32
μ	0.85	0.75	1.94	0.90
m_g	**0.27***	0.22	**1.25***	**0.46***
m_v	0.09	0.06	**0.71‡**	0.16
PRO				
μ_{env}	1.63	0.76	—	0.60
μ	1.56	−0.02	—	0.56
m_g	**0.90***	0.06	—	**0.58***
m_v	0.05	0.25	—	−0.19
SYN				
μ_{env}	0.00	0.42	1.10	0.27
μ	0.30	0.36	1.24	0.53
m_g	**0.27***	−0.05	−0.01	**0.30***
m_v	0.07	**0.44***	**0.55***	0.14
PEUK				
μ_{env}	0.02	0.43	0.76	0.42
μ	0.29	0.23	0.93	0.45
m_g	0.05	**0.35***	**0.68***	**0.53***
m_v	**0.52‡**	−0.37	−0.07	−0.32

In situ growth rates (μ_{env}), are the corrected growth rates based on the net growth (k) in non-nutrient addition incubation bottles (see the Method section) and are the growth rates referred to throughout the Results and Discussion sections, but μ (i.e. the uncorrected intercept for each experiment) is also provided below. The value for μ provided is from the dilution series (0.1 μm versus 30 kDa) with the greater intercept (e.g. the highest growth rate detected in the absence of mortality sources). This value is from the 0.1 μm dilution series for all but the following cases: PEUK Experiment 1, PRO and SYN Experiment 2, SYN and Experiment 3, SYN Experiment 4. Mortality estimates are for grazing (m_g) and viral lysis (m_v), respectively. Bold values indicate significant mortality rates (*$\alpha = 0.05$; ‡$\alpha = 0.10$).

Based on chlorophyll *a*, the autotrophic community had the highest growth rate on the cold, nitrate-rich side of the front during Experiment 3 (0.79 day^{-1}) and the lowest rates in Experiments 2 and 4 (0.35 day^{-1} in Experiment 2 offshore and 0.32 day^{-1} in Experiment 4 on the warm side of the front) (Table III). During Experiment 3, significant grazer and viral mortalities were detected (1.25 day^{-1}, *P*-value = 0.0003; 0.71 day^{-1}, *P*-value = 0.10, respectively), whereas only grazing mortality was significant for Experiments 1 and 4 (0.27 day^{-1}, *P*-value = 0.006 and 0.46 day^{-1}, *P*-value = 0.0004, respectively). For Experiment 2, no significant mortality was detected.

Estimated growth rates were higher for PRO than for the other picophytoplankton in all experiments (Table III), but no significant viral mortality was detected for PRO. Significant grazing mortality of PRO was determined for Experiments 1 and 4 (0.90 day^{-1}, *P*-value <0.0001 and 0.58 day^{-1}, *P*-value <0.0001, respectively), but not for Experiment 2. Growth and grazing rates were balanced in Experiment 4, but growth exceeded mortality for Experiments 1 and 2, resulting in net growth of ~0.7 day^{-1}.

Growth rates of SYN were highest for Experiment 3 (1.1 day^{-1}) and lowest for Experiment 1 (~zero). Viral mortality was detected in all experiments, but was only significant for Experiments 2 and 3 (0.44 day^{-1}, *P*-value = 0.004 and 0.55 day^{-1}, *P*-value = 0.01, respectively) (Table III). Where viral lysis was significant (Experiments 2 and 3), grazing mortality was not. Grazing mortality was ~0.30 day^{-1} for Experiments 1 and 4 (*P*-values = 0.0001 and 0.002, respectively).

For PEUKs, growth rates were highest for Experiment 3 (0.76 day^{-1}) and similar for Experiments 2 and 4 (0.43 and 0.42 day^{-1}, respectively) (Table III). PEUK growth was suppressed in the viral dilution series (30 kDa filtrate) for Experiments 2 and 4, but neither was statistically significant. Growth and grazing were fairly well balanced for PEUKs, except for Experiment 1 where viral mortality was significant (0.52 day^{-1}, *P*-value = 0.06) and exceeded growth.

Overall, grazing mortality and viral lysis rates were inversely related across all picophytoplankton populations in each experiment (Fig. 4). This pattern remained consistent, even though the source and magnitude of mortality for individual populations varied across experiments (Fig. 4). For all populations and experiments combined, we also observed a significant negative relationship between grazing and viral lysis ($R^2 = 0.48$, Fig. 5).

Heterotrophic bacteria

Heterotrophic bacterial growth rates were higher during Experiment 1 relative to Experiment 2 (0.44 and 0.07

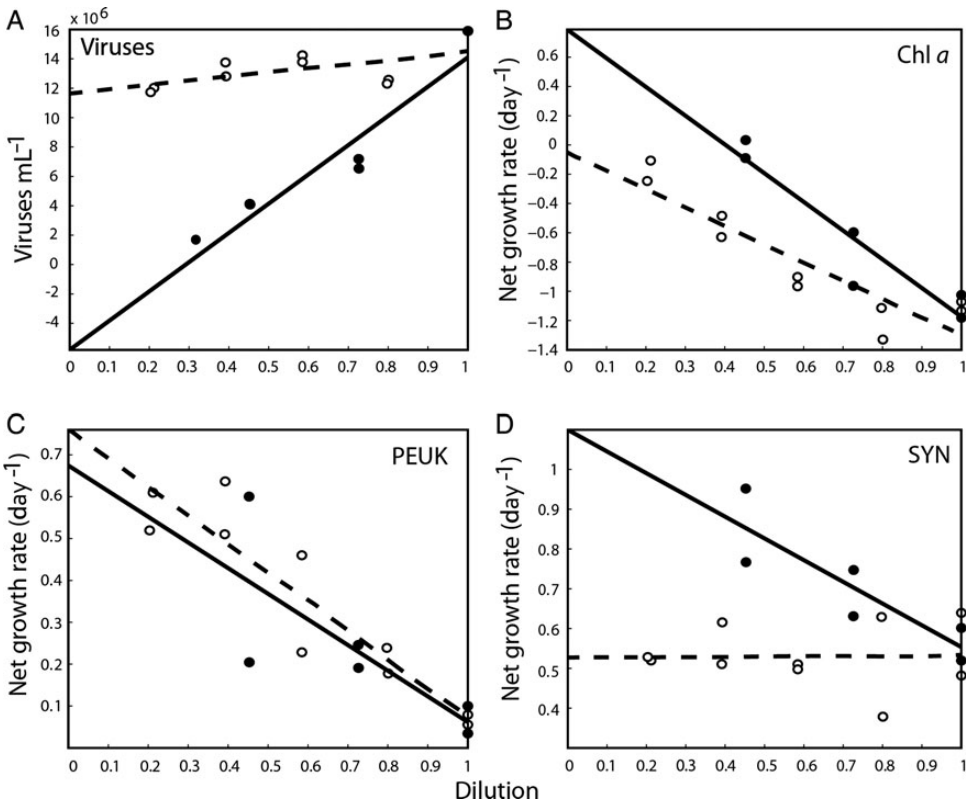

Fig. 3. (**A**) Virus concentration at the start of Experiment 3 showing a reduction in viruses across the 30 kDa dilution series (closed symbols) relative to the 0.1 μm-dilution series (open symbols). (**B**–**D**) Net growth rate (day^{-1}) versus fraction of natural seawater (dilution) from Experiment 3 based on chlorophyll *a*, SYN and PEUK. Open and closed circles represent growth rates in the 0.1 μm and 30 kDa dilution series, respectively. Dashed and solid lines represent linear regressions of data from the 0.1 μm and 30 kDa dilution series, respectively. See Table III for statistical significance for all experiments. Corresponding regression equations for dilution series: chlorophyll *a* (B) $y = -1.25x - 0.05$ (0.1 μm series), $y = -1.96x + 0.79$ (30 kDa series); PEUK (C) $y = -0.68x + 0.76$ (0.1 μm series), $y = -0.61x + 0.67$ (30 kDa series); SYN (D) $y = 0.006x + 0.53$ (0.1 μm series), $y = -0.55x + 1.1$ (30 kDa series).

day^{-1}, respectively; Table IV). Growth rates across the front followed the same pattern as the inshore versus offshore sites, but they were higher (2.22 day^{-1} for Experiment 3 and 0.36 day^{-1} for Experiment 4). Assuming a bacterial carbon conversion factor of 11 fg C $cell^{-1}$ (Garrison *et al.*, 2000), dilution growth rates can be converted to bacterial carbon production (BCP) of 12.0 and 2.8 μg C L^{-1} day^{-1} for Experiments 3 and 4, respectively. Independent measurements of BCP across the front (1 h leucine incorporation; details in Samo *et al.*, 2012) resulted in BCP estimates of 12.8 ± 1.4 and 1.5 ± 0.02 μg C L^{-1} day^{-1} for the sampling locations of Experiments 3 and 4, respectively. These independent assessments of BCP suggest that the estimated bacterial growth rates from the 0.1 μm dilution series reasonably reflect their growth dynamics during our study. Heterotrophic bacterial growth was significantly suppressed in the viral dilution series (30 kDa filtrate) relative to the traditional dilution series (0.1 μm filtrate) during Experiment 1 (*P*-value = 0.05) and Experiment 3 (*P*-value = 0.008; Table IV and Supplementary data, Fig. S2). Significant growth suppression was not detected for Experiments 2 and 4. Figure 6 shows a schematic of the potential outcomes of the modified dilution method, including a visualization of the growth suppression described above.

DISCUSSION

Our experiments reveal three main results. First, we observed diverse mortality impacts for the populations examined within individual experiments. This result is particularly notable for grazing mortality, where despite recent laboratory studies demonstrating grazer selectivity on prey within a narrow size range (0.5–3 μm) (e.g. Apple *et al.*, 2011), there are still limited data from natural communities to support this notion. This is relevant to efforts that seek to model plankton community dynamics based only on size-structured growth and

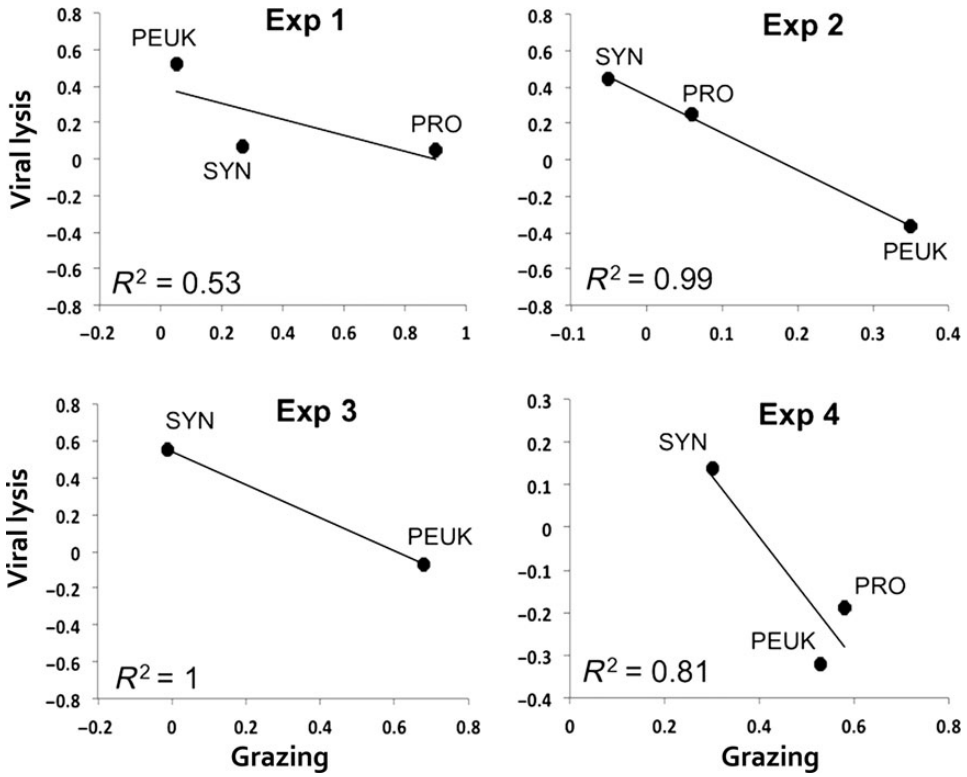

Fig. 4. Relationship between viral lysis (day^{-1}) and grazing (day^{-1}) within each of the modified dilution experiments in the CCE. R^2 value represents the proportion of the data explained by the linear regression (black line).

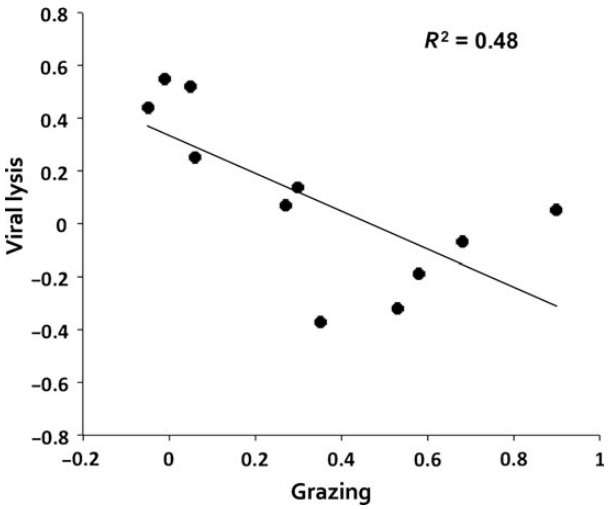

Fig. 5. Relationship between viral lysis (day^{-1}) and grazing (day^{-1}) across all of the modified dilution experiments in the CCE. R^2 value represents the proportion of the data explained by the linear regression (black line).

grazing (e.g. Poulin and Franks, 2010; Ward *et al.*, 2012, 2014). We also observed, particularly for the heterotrophic bacteria, a negative response of net growth rate to dilution with 30 kDa filtrate relative to 0.1 μm filtrate. The implications of altering the growth dynamics of heterotrophic bacteria are typically ignored in this type of experiment, but may be important. Finally, we found an inverse relationship between estimates of grazing and viral mortality within and across all of our experiments. This suggests that there is a relationship between grazing and viral mortality agents, or at least that a relationship exists between processes that affect the dynamics of picoplankton populations in ways that appear to be mortality linked. Below, the results of these experiments are considered not only in terms of ecological and biogeochemical significance, but also in terms of methodological implications.

Table IV: Growth rates (day^{-1}) of heterotrophic bacteria in the 0.1 μm ($\mu_{0.1\mu m}$) and 30 kDa (μ_{30kDa}) dilution series

	Exp. 1	Exp. 2	Exp. 3	Exp. 4
$\mu_{0.1\mu m}$	0.44	0.07	2.22	0.36
$\mu_{30\ kDa}$	−0.26	−0.08	1.55	0.37

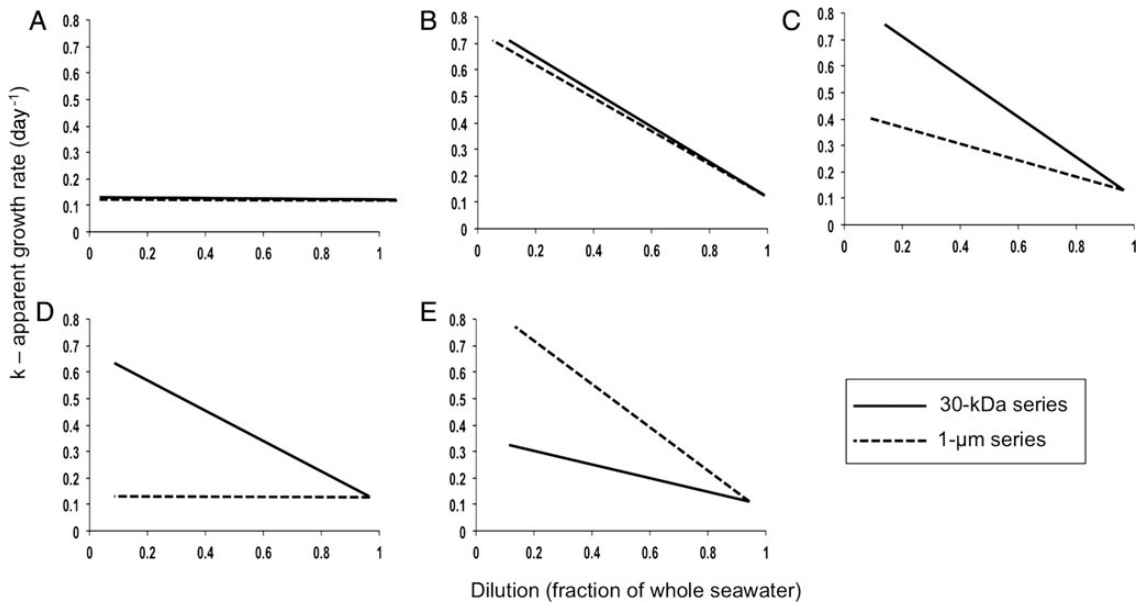

Fig. 6. Schematic of the different potential outcomes during the modified dilution method. The 0.1 μm series is diluted with water containing viruses but no grazers and the 30 kDa dilution series is diluted with viral-free and grazer-free water. (**A**) No significant grazer or viral mortality detected (i.e. the lines are not significantly different from zero). (**B**) Significant grazer mortality, but no significant viral mortality detected (i.e. the lines are not significantly different from one another, but are significantly different from zero). (**C**) Significant grazer and viral mortality detected (i.e. the lines are significantly different from zero and they are significantly different from one another). This is the idealized case in which after removing both sources of morality in the 30 kDa series, a higher growth rate of the population is observed. (**D**) No grazer mortality, but significant viral mortality detected (i.e. the 0.1 μm series line is not significantly different from zero, but the 30 kDa series is significantly different from zero and the grazer line). (**E**) Significant grazer mortality and negative viral mortality (i.e. the removal of viruses reduced the growth of the population relative to the 0.1 μm series either as a result of methodological complications or ecological consequences).

Impacts of viral lysis and grazing on picophytoplankton communities

We undertook the present experiments, in part, to assess the magnitude of phytoplankton growth potential that may have been missed in previous CCE studies that did not consider viral losses (Landry *et al.*, 2009). From chlorophyll-based community results in which only one of four experiments registered a measurable viral mortality effect (at $P = 0.1$), the answer is nonetheless substantial. On average, phytoplankton growth rate was $0.26 \pm 0.31\text{day}^{-1}$ higher when including the viral impact. Consistently among experiments, the inclusion of this impact enhanced total microbial mortality of the phytoplankton assemblage by $\sim 38 \pm 13\%$ relative to protistan grazing alone (i.e. $(m_g + m_v)/m_g = 1.38 \pm 0.13$; range $1.27-1.57$). As considered below, quantifying the population-specific effects is more complicated.

The picophytoplankton populations examined in this study exhibited a range of growth and mortality dynamics. For PEUKs, grazing was the dominant source of mortality in all experiments except Experiment 1 (closest to shore), where viral mortality was significant. Because PEUKs were more abundant at this site relative to the others, enhanced viral mortality during this experiment is consistent with the expected dependency of viral lysis rate on host density (Jacquet *et al.*, 2002). Using the same modified dilution method, Baudoux *et al.* (Baudoux *et al.*, 2008) also found that most mortality of PEUKs in the North Sea was due to grazing, except at a coastal sampling site where viral lysis was high. At this site, Baudoux *et al.* (Baudoux *et al.*, 2008) observed elevated abundance of a particular group of picoeukaryotes, the prasinophytes. Concentrations of viruses that infect prasinophytes (e.g. *Micromonas pusilla*) are typically higher in nearshore relative to offshore regions (Cottrell and Suttle, 1991; Baudoux *et al.*, 2008). Together, these studies suggest that not only host concentrations, but also composition may influence picoeukaryote viral mortality dynamics.

On the other hand, viral mortality of SYN was correlated with its growth rate ($R^2 = 0.86$, data shown in Table III) rather than cell concentration. This is consistent with the model proposed by Proctor and Fuhrman (Proctor and Fuhrman, 1990) based on the number of visibly infected cells. Positive relationships between host growth rate and viral lysis have also been demonstrated for other groups of organisms in both the laboratory and field (e.g. Bratbak *et al.*, 1998; Middelboe, 2000; Baudoux

et al., 2007). It is therefore intriguing to speculate that rapid growth of hosts may often serve to increase the activity of their viruses. However, the amount of SYN production that goes through the viral shunt is dependent on the ratio of m_v/μ_{env}. While on average, 67% of SYN production was cycled through the viral shunt, individual experimental variability ranged from 50 to >100%. Since particulate organic material exported to deeper waters by the viral shunt is thought to be more carbon rich than the material from which it was derived (Suttle, 2007), the biogeochemical consequences of such a growth–lysis relationship could be substantial. In the present case, however, interpretation may be confounded by the presence of different clonal types of SYN in the southern CCE (Tai *et al.*, 2011), each with likely different growth characteristics and viral susceptibilities (Suttle and Chan, 1993). Future studies in this region should monitor the different strains of SYN and other picophytoplankton to determine the differential influences of viral mortality on specific strains.

The net growth rate of PRO for both the inshore and offshore populations was $\sim 0.7 day^{-1}$; therefore, measurable changes in total abundance over time were similar for PRO in each of these environments. However, the instantaneous growth rate of the inshore PRO population was double that of the growth rate of the offshore PRO population. It was only because the inshore population also had a higher mortality rate that a similar net growth rate was observed. No significant viral mortality was detected for PRO during our experiments. At least for PRO, viruses may play a larger role in diversity maintenance of the assemblage rather than cause net declines in total abundance. Abundant PRO populations belonging to a single ecotype with common physiological and ecological characteristics are hypothesized to be an assortment of subpopulations with different susceptibilities to co-occurring viruses (Avrani *et al.*, 2011). A high diversity of viral attachment genes in PRO populations results in a genomic mechanism that reduces the effective host population size for infection by a specific virus (Avrani *et al.*, 2011), thereby enabling the coexistence of PRO and its viruses.

While viruses and grazers can both exert significant mortality impacts on microbial communities, viral lysis is considered highly selective and more likely to control species diversity while grazing is generally associated with bulk consumption that regulates biomass (e.g. Thingstad, 1998; Pedros-Alio *et al.*, 2000). Although controlled laboratory experiments have demonstrated pronounced variability in microbial grazing defenses among clones of the same prey species or comparably sized species of the same genus (e.g. Monger *et al.*, 1999; Strom *et al.*, 2003, 2012; Boenigk *et al.*, 2004; Apple *et al.*, 2011), differential grazing vulnerability and selective grazing are poorly explored in natural systems. In the present experiments under variable environmental conditions in the CCE region, we see grazing mortality rate differences among microbial populations up to $1.2 day^{-1}$ (Experiments 1 and 3). We hypothesize that this variability in grazing impact may reflect site differences in population-specific grazing defenses. The consequences of particular tradeoffs in grazer and virus resistance strategies are explored in the discussion section *Interaction of grazers and viral lytic impacts*.

Size-structured plankton food-web models are often used to explain and predict spatial and temporal variability in planktonic communities (Ward *et al.*, 2012, 2014). While some field studies support the notion that all prey in a particular size range suffer similar proportional grazing losses regardless of their component populations, others, including this study, show contradictory results. Under the relatively steady-state conditions of the eastern equatorial Pacific, for example, the turnover rates of PRO, SYN and PEUK due to protistan grazing are similar (40–50% of biomass day^{-1}; Landry *et al.*, 2011), despite greater than order of magnitude differences in prey biomasses and cell abundances that would presumably lead to larger population-specific differences in encounter frequencies and viral infections. However, a recent regional comparison showed a lack of size-dependent trends in grazing vulnerability within the picophytoplankton size range (Taniguchi *et al.*, 2014). To model variability in planktonic community structure accurately, it is imperative to better understand the predator–prey relationships influencing mortality alongside size-dependency factors.

Exploring manipulation consequences on picoplankton communities

The dilution method relies on the sequential dilution of a natural community with filtered seawater to reduce the predator–prey encounter rate, thereby allowing simultaneous measurement of phytoplankton growth and microzooplankton grazing. There are three main assumptions to the dilution method: phytoplankton growth is exponential, phytoplankton growth is not affected by dilution and the probability of a phytoplankton cell being consumed is a linear function of predator encounter rate. Previous studies in the CCE have demonstrated that standard dilution experiments produce reliable rate estimates of phytoplankton growth and microzooplankton grazing, as judged by their ability to predict the observed net rates of phytoplankton growth in ambient water parcels tracked by drifters (Landry *et al.*, 2009) and their effectiveness in trophic models for predicting measured rates of carbon export (Stukel *et al.*, 2011). The modified dilution method has not previously been applied in a dynamic region like

the CCE, nor have the assumptions of the modified dilution method been explored as extensively as the dilution grazing rate estimates.

There are many potential methodological constraints of the modified dilution method (Table V, see Supplementary data for more details), some of which have been previously addressed by Jacquet *et al.* (Jacquet *et al.*, 2005) and Kimmance *et al.* (Kimmance *et al.*, 2007). One particular issue that has not been previously addressed is the response of heterotrophic bacteria to manipulation. In Experiments 1 and 3, we observed a significant decrease in heterotrophic bacterial growth rate in the 30 kDa series relative to the 0.1 μm series (Table IV and Fig. 6E). Independent estimates of BCP suggest that the growth rates derived from the 0.1 μm series accurately reflected heterotrophic bacterial growth during our experiments. We make no attempt to extract grazing or viral mortality estimates of heterotrophic bacteria from these experiments. But rather than interpret these results as failed experiments, it is important to understand what happened to the heterotrophic bacteria, hypothesize why lower growth rates were observed in the 30 kDa series and consider how this could affect interpretation of results for other populations.

Lower net growth rates in 30 kDa dilution series relative to the 0.1 μm dilution series may have an ecological interpretation, assuming the presence of viruses is beneficial, either because they reduce competition by lysing other populations or enhance growth indirectly by remineralizing material required for growth. Mesocosm studies in the CCE region have demonstrated that heterotrophic bacteria are about equally vulnerable to mortality from viruses and grazers (Fuhrman and Noble, 1995). Although viral stimulation of bacterial growth rate is consistent with predictions of dissolved organic cycling from simple food-web models (e.g. Fuhrman, 1992), given the relatively high respiratory cost and low efficiency of bacterial growth (Anderson and Ducklow, 2001), the net effect of viral lytic cycling on bacterial biomass is unlikely to be consistently positive, unless perhaps if the released resource is critically limiting for growth and not otherwise available.

Reduced growth rates of heterotrophic bacteria in 30 kDa water can also be interpreted as a methodological consequence of microbial community manipulation. The suite of DOM available to heterotrophic bacteria could be a major difference between the two dilution series. Dilution with 30 kDa filtrate could, for example, reduce resources that contribute significantly to heterotrophic bacterial growth on the time scale of 24 h experiments. We speculate that such resources may reside in the colloidal and high-molecular-weight fraction of dissolved organic material, which are believed to be more labile and easily utilized than smaller DOM molecules (Smith *et al.*, 1992; Amon and Benner, 1994, 1996; Gómez-Consarnau *et al.*, 2012). The pattern of growth suppression observed across the experiments supports this possibility. Significantly, lower heterotrophic bacterial growth rates were observed only in the 30 kDa dilution series during Experiments 1 and 3, which had the highest concentrations of POC, PON and chlorophyll *a*. Heterotrophic bacterial growth rates across our experiments were highly correlated with both POC ($R^2 = 0.99$) and chlorophyll *a* concentration ($R^2 = 0.98$) (data shown in Tables I and IV). Higher POC concentrations are indicative of higher rates of primary production and have been shown to be positively correlated with bacterial growth rates, BCP, and bacterial growth efficiency (BGE) (del Giorgio and Cole, 1998). It has further been hypothesized that intense hydrolytic enzyme activity on marine particles may be an important source of DOM (Smith *et al.*, 1992). Attached bacteria may play a large role in particle decomposition (Cho and Azam, 1998); thereby creating localized regions of high concentrations of DOM for free-living bacteria. Heterotrophic bacterial populations living in these environments were likely adapted to high POC conditions and a particular suite of dissolved carbon degradation products (Smith *et al.*, 1992; Gómez-Consarnau *et al.*, 2012). By manipulating the community through dilution with 30 kDa filtrate, this close coupling between bacteria and their growth-sustaining substrates was likely disrupted. We did not observe significant suppression of growth in oligotrophic waters (Experiments 2 and 4), which had lower POC concentrations and presumably different bacteria adapted to these conditions and specific dissolved carbon degradation products (Gómez-Consarnau *et al.*, 2012).

Another important consideration for interpreting modified dilution results is that significant effects may arise as indirect consequences of reduced viral-induced mortality and altered heterotrophic bacterial growth dynamics. In experimental incubations, Weinbauer *et al.* (Weinbauer *et al.*, 2011) and Shelford *et al.* (Shelford *et al.*, 2012) have shown that viruses enhance the growth rates of *Synechococcus* and the phytoplankton community, respectively. Both studies attribute these results to indirect effects of viral lysis of heterotrophic bacteria. Shelford *et al.* (Shelford *et al.*, 2012) further linked viral enhancement of phytoplankton growth to increased release of ammonium, which is hypothetically the remineralized product of dissolved organics released from virally lysed bacteria by the assemblage of uninfected bacteria. If SYN relies on heterotrophic bacteria directly or indirectly, SYN growth may be underestimated by altering these interactions (Malfatti and Azam, 2009).

Based on the patterns of heterotrophic bacteria in response to dilution, how then do we interpret reduced

Table V: Summary of the potential methodological limitations of the modified dilution method for assessing viral mortality in natural populations

Dilution method assumption (based on Landry and Hassett, 1982)	Limitation for application to virus/prey dynamics	Details	Potential solution/modification
Probability of a prey cell being consumed is a direct function of the encounter rate with predator	Previously infected cells	As a result of previously infected cells, some cell lysis may be the result of infections that occurred prior to incubation and therefore not influenced by dilution. However, depending on the timing of infection relative to the course of the experiment, some infection events that occur during the incubation may not result in lysis	Quantify the number of visibly infected cells at the beginning and end of the experiment to estimate the fraction of the population this impacts
	Length of infection cycle relative to incubation time	Prior to measuring any biological rate, it is necessary to determine the appropriate experimental time required to capture a particular process. For 24 h modified dilution experiments, only mortality caused by viruses with lytic cycles $<$24 h will be captured. Note: This approach misses the mortality impact of viruses with long lytic cycles as well as lysogenic viruses	Vary length of experiment to capture a range of temporal dynamics
	Density-dependent predator–prey dynamics	Prey threshold concentrations may result in non-linear mortality dynamics	Assess whether non-linear responses are observed in experimental results
Phytoplankton growth is independent of dilution	Phytoplankton growth	Phytoplankton growth rates may be influenced by dilution if the phytoplankton become limited by nutrients. Additionally, if the growth of a population relies on viral lysis of other populations (due to nutrient cycling or reduction in competition), the reduction in viral mortality through dilution may influence growth dynamics	(i) Quantify photosynthetic efficiency (F_v/F_m) of phytoplankton populations to confirm the phytoplankton do not exhibit signs of stress. (ii) In waters where nutrient limitation may be suspected, add nutrients to reduce the influence of dilution on phytoplankton growth
	Heterotrophic bacterial growth	Different filtration cut-offs between the 0.1 μm and 30 kDa dilution series influence the suite of dissolved organic matter available in the incubation bottles	(i) Use an additional method to measure heterotrophic bacterial growth (e.g. leucine incorporation) for comparison. (ii) Monitor changes in the heterotrophic bacterial population in the most dilute bottles over time (e.g. *k*) to determine if growth in the 30-kDa series is reduced. (iii) Use method in low POC areas where heterotrophic bacterial populations are not adapted to freshly produced degradation products (e.g. colloids and high molecular weight DOC)
Ability to detect viral mortality[a]	Limits of detection in terms of statistics	In some cases, rates of viral mortality may occur below the limits of detection of the dilution method	Perform sensitivity analysis to determine the effect size (e.g. viral mortality rate) that can be captured
	Limits of detection in terms of bulk population measurements	Since viral mortality is thought to work at the species level rather than the bulk community level, viral-mediated mortality may not be detected when measuring changes in total population abundances over time	(i) Limit use of method for capturing bloom dynamics when one dominant population maybe subject to high viral mortality. (ii) Measure changes at the species level rather than bulk population level

[a]This is not exclusively an assumption of the dilution method; however, it is important to have the ability to measure the biological phenomenon of interest.

picophytoplankton growth rates in response to 30 kDa dilution? Although the measured viral mortality rates are not statistically significant, we observed lower growth rates (Fig. 6E) for PEUK in Experiments 2 and 4, the oligotrophic offshore stations where ambient nutrients are low. The elevated rates of viral mortality of PRO and SYN in Experiment 2 imply that benefit to PEUK could come at the expense of lysing the presumptively more efficient competitors for limiting resources (Table III). However, this inverse rate pattern between eukaryotic and prokaryotic picophytoplankton is not supported by measurements from Experiment 4. Further work is needed to understand how dilution alters interactions over a broader range of environmental conditions in order to distinguish between ecological and methodological interpretations of experimental results.

Interactions of grazer and viral lytic impacts

Perhaps the most striking result of the present study is that despite high variability in the responses of individual populations, there emerge consistent and significant inverse relationships between grazing and viral lysis both within individual experiments and across all experiments spanning a range of environmental conditions and grazing pressures. The inverse relationship does not appear to change with variations in community structure and system productivity. Such results could arise from either direct or indirect interactions among grazers and viruses (e.g. Šimek *et al.*, 2001; Weinbauer *et al.*, 2007; Miki and Jacquet, 2008).

While direct interactions among protistan grazers and viruses have been documented, their significance in natural marine ecosystems is not well understood. Laboratory studies have demonstrated that nanoflagellates (Gonzalez and Suttle, 1993) and ciliates (Pinheiro *et al.*, 2007) can consume and digest marine viruses, but the rates extrapolated to natural abundances are low ($\leq$0.3% day^{-1}, Baudoux *et al.*, 2007). In a more concentrated freshwater environment, however, concurrent changes in grazer abundance and viral size structure have been interpreted as evidence for significant direct consumption of viruses by grazers (Demuth *et al.*, 1993; Weinbauer, 2004). Direct viral-induced mortality of grazers has also been observed in a few instances (Garza and Suttle, 1995; Massana *et al.*, 2007). While the prevalence of this interaction in natural systems is largely unstudied, it is unlikely that the viruses infecting picophytoplankton are sufficiently well coordinated with the viruses infecting the grazers of those same picophytoplankton to explain the observed inverse relationship between grazing and lysis.

Indirect interactions among grazers and viruses may be important if viral infections make cells more susceptible to grazers or if there are tradeoffs in the grazing and virus resistance strategies of picoplankton such that they cannot both be maximally effective at the same time. There is evidence to support both mechanisms. For example, Evans and Wilson (Evans and Wilson, 2008) documented increased protistan grazing on virally infected cells of *Emiliania huxleyi*, implying that the physiological changes experienced by the cells during viral infection (e.g. increased cell size, changes in nucleic acid content or variability in the magnitude and type of exudation products; Brussaard *et al.*, 2001; Evans *et al.*, 2006, 2007) make them more susceptible to grazers. Experimental studies with *Synechococcus* show selection for phage resistance when viral concentration is high (Waterbury and Valois, 1993; Suttle, 2000), and indicate that cell surface properties reducing viral infection may increase grazing vulnerability (Zwirglmaier *et al.*, 2009). Given these indirect mechanisms for viral–grazer interactions, spatially separated populations might therefore exhibit inverse variability in grazing and viral lytic effects, with significant differences in phasing of grazing and viral resistance among different populations in the same water parcel. Such results would be consistent with our experimental rate measurements. However, we cannot rule out the possibility that some of the observed grazing variability resulted from differential sensitivities of the site-specific protistan communities to dilution (Dolan *et al.*, 2000; Dolan and McKeon, 2005; Modigh and Franzè, 2009).

The observed variability in responses of individual prey/host populations in our study highlights the complexity of community interactions in marine ecosystems. The fact that consistent and significant inverse relationships between grazing and viral lysis effects can be observed, despite this variability suggests that direct and indirect interactions between grazer and virus mortality agents may be significant enough in natural systems to impact the dynamics of populations and regulate community diversity. Clarifying and testing the mechanisms that drive such interactions are important goals for future research.

SUPPLEMENTARY DATA

Supplementary data can be found online at http://plankt.oxfordjournals.org.

ACKNOWLEDGEMENTS

We are grateful to the captain and crew of the R/V Melville and to all participants who contributed to the success of the CCE-LTER October 2008 process cruise. In particular, we thank Ian Ball and Lihini Aluwihare for TOC data, Ralph Goericke for POC and PON data, Ali

Friebott and Lorena Linacre for ciliate counts, Andrew Taylor and John Wokuluk for epifluorescence microscopy and Karen Selph for flow cytometry data. Interpretation of experimental viral effects benefited from discussions with Curtis Suttle and Hongbin Liu.

FUNDING

This project was supported by National Science Foundation (NSF) funding (OCE 0417616 and 1026607) for the CCE LTER site and by an NSF Graduate Research Fellowship to A.L.P.

REFERENCES

Allen, L. Z., Allen, E. A., Badger, J. H. *et al*. (2012) Influence of nutrients and currents on the genomic composition of microbes across an upwelling mosaic. *ISME J.*, **6**, 1403–1414.

Amon, R. M. W. and Benner, R. (1994) Rapid cycling of high-molecular-weight dissolved organic matter in the ocean. *Nature*, **369**, 549–552.

Amon, R. M. W. and Benner, R. (1996) Bacterial utilization of different size classes of dissolved organic matter. *Limnol. Oceanogr.*, **41**, 41–51.

Anderson, T. R. and Ducklow, H. W. (2001) Microbial loop carbon cycling in ocean environments studied using a simple steady-state model. *Aquat. Microb. Ecol.*, **26**, 37–49.

Andersen, T., Schartau, A. K. L. and Paasche, E. (1991) Quantifying external and internal nitrogen and phosphorous pools, as well as nitrogen and phosphorous supplied through remineralization, in coastal marine plankton by means of the dilution technique. *Mar. Ecol. Prog. Ser.*, **69**, 67–80.

Apple, J. K., Strom, S. L., Palenik, B *et al*. (2011) Variability in protists grazing and growth on different marine *Synechococcus* isolates. *Appl. Environ. Microbiol.*, **77**, 3074–3084.

Avrani, S., Wurtzel, O., Sharon, I. *et al*. (2011) Genomic island variability facilitates *Prochlorococcus*-virus coexistence. *Nature*, **474**, 604–608.

Baudoux, A. C., Veldhuis, M. J. W., Noordeloos, A. A. M. *et al*. (2008) Estimates of virus- vs. grazing induced mortality of picophytoplankton in the North Sea during summer. *Aquat. Microb. Ecol.*, **52**, 69–82.

Baudoux, A. C., Veldhuis, M. J. W., Witte, H. J. *et al*. (2007) Viruses as mortality agents of picophytoplankton in the deep chlorophyll maximum layer during IRONAGES III. *Limnol. Oceanogr.*, **52**, 2519–2529.

Boenigk, J., Stadler, P., Wiedlroither, A. *et al*. (2004) Strain-specific differences in the grazing sensitivities of closely related ultramicrobacteria affiliated with the Polynucleobacter cluster. *Appl. Environ. Microbiol.*, **70**, 5787–5793.

Bratbak, G., Jacobsen, A., Heldal, M. *et al*. (1998) Virus production in *Phaeocystis pouchetii* and its relation to host cell growth and nutrition. *Aquat. Microb. Ecol.*, **14**, 1–9.

Brink, K. H. and Cowles, T. J. (1991) The coastal transition zone program. *J. Geophys. Res.*, **96**, 14637–14647.

Brussaard, C. P. D. (2004) Viral control of phytoplankton populations—a review. *J. Eukaryot. Microbiol.*, **51**, 125–138.

Brussaard, C. P. D., Marie, D., Thyrhaug, R. *et al*. (2001) Flow cytometric analysis of phytoplankton viability following viral infection. *Aquat. Microb. Ecol.*, **26**, 157–166.

Calbet, A. and Landry, M. R. (2004) Phytoplankton growth, microzooplankton grazing, and carbon cycling in marine systems. *Limnol. Oceanogr.*, **49**, 51–57.

Checkley, D. M. and Barth, J. A. (2009) Patterns and processes in the California Current System. *Prog. Oceanogr.*, **83**, 49–64.

Cho, B. C. and Azam, F. (1998) Major role of bacteria in biogeochemical fluxes in the ocean's interior. *Nature*, **332**, 441–443.

Cottrell, M. T. and Suttle, C. A. (1991) Wide-spread occurrence and clonal variation in viruses which cause lysis of a cosmopolitan eukaryotic marine phytoplankton, *Micromonas pusilla*. *Mar. Ecol. Prog. Ser.*, **78**, 1–9.

del Giorgio, P. A. and Cole, J. J. (1998) Bacterial growth efficiency in natural aquatic systems. *Ann. Rev. Ecol. Syst.*, **29**, 503–541.

Dolan, J. R. and McKeon, K. (2005) The reliability of grazing rate estimates from dilution experiments: Have we over-estimated rates of organic carbon consumption by microzooplankton?. *Ocean Sci.*, **1**, 1–7.

Dolan, J. R., Gallegos, C. L. and Moigis, A. (2000) Dilution effects on microzooplankton in dilution grazing experiments. *Mar. Ecol. Prog. Ser.*, **200**, 127–139.

Demuth, J., Neve, H. and Witzel, K. P. (1993) Direct electron microscopy study on the morphological diversity of bacteriophage populations in Lake Plußsee. *Appl. Environ. Microbiol.*, **59**, 3378–3384.

Evans, C., Archer, S. D., Jacquet, S. *et al*. (2003) Direct estimates of the contribution of viral lysis and microzooplankton grazing to the decline of a *Micromonas spp.* population. *Aquat. Microb. Ecol.*, **30**, 207–219.

Evans, C. and Brussaard, C. P. D. (2012) Viral lysis and microzooplankton grazing of phytoplankton throughout the Southern Ocean. *Limnol. Oceanogr.*, **57**, 1826–1837.

Evans, C., Kadner, S. V., Darroch, L. J. *et al*. (2007) The relative significance of viral lysis and microzooplankton grazing as pathways of dimethylsulfoniopropionate (DMSP) cleavage: an *Emiliania huxleyi* culture study. *Limnol. Oceanogr.*, **52**, 1036–1045.

Evans, C., Malin, G., Mills, G. P. *et al*. (2006) Viral infection of *Emiliania huxleyi* (Prymnesiophyceae) leads to elevated production of reactive oxygen species. *J. Phycol.*, **42**, 1040–1047.

Evans, C. and Wilson, W. H. (2008) Preferential grazing of *Oxyrrhis marina* on virus-infected *Emiliania huxleyi*. *Limnol. Oceanogr.*, **53**, 2035–2040.

Freibott, A., Linacre, L. and Landry, M. R. (2014) A slide preparation technique for light microscopy analysis of ciliates preserved in acid Lugol's fixative. *Limnol. Oceanogr. Meth.*, **12**, 54–62.

Fuhrman, J. A. (1992) Bacterioplankton roles in cycling of organic matter: The microbial food web. In Falkowski, P. G. and Woodhead, A. D. (eds), *Primary Productivity and Biogeochemical Cycles in the sea. Environmental Science Research*, vol. 43. Springer, USA, pp. 361–383.

Fuhrman, J. A. (1999) Marine viruses and their biogeochemical and ecological effects. *Nature*, **399**, 541–548.

Fuhrman, J. A. and Azam, F. (1980) Bacterioplankton secondary production estimates for coastal waters of British Columna, Antarctica, and California. *Appl. Environ. Microbiol.*, **39**, 1085–1095.

Fuhrman, J. A. and Noble, R. T. (1995) Viruses and protists cause similar bacterial mortality in coastal seawater. *Limnol. Oceanogr.*, **40**, 1236–1242.

Garrison, D. L., Gowin, M. M., Hughes, M. P. *et al*. (2000) Microbial food web structure in the Arabian Sea: a US JGOFS study. *Deep-Sea Res. II*, **47**, 1387–1422.

Garza, D. R. and Suttle, C. A. (1995) Large double-stranded DNA viruses which cause the lysis of a marine heterotrophic nanoflagellate (*Bodo* sp.) occur in natural marine viral communities. *Aquat. Microb. Ecol.*, **9**, 203–210.

Gómez-Consarnau, L., Lindh, M. V., Gasol, J. M. *et al.* (2012) Structuring of bacterioplankton communities by specific dissolved organic compound. *Environ. Microbiol.*, **14**, 2361–2378.

Gonzalez, G. M., Sherr, E. B. and Sherr, B. F. (1990) Size-selective grazing on bacteria by natural assemblages of estuarine flagellates and ciliates. *Appl. Environ. Microbiol.*, **53**, 583–589.

Gonzalez, J. M. and Suttle, C. A. (1993) Grazing by marine nanoflagellates on viruses and viral-sized particles: ingestion and digestion. *Mar. Ecol. Prog. Ser.*, **94**, 1–10.

Gordon, L. I., Jennings, J. C., Ross, A. A. *et al.* (1993) A suggested protocol for continuous flow automated analysis of seawater nutrients in the WOCE hydrographic program and the Joint Global Ocean Fluxes Study. Grp Tech Rpt 92-1, OSU College of Oceanography Descriptive Chem Oc.

Hansen, P. J., Bjørnsen, P. K. and Hansen, B. W. (1997) Zooplankton grazing and growth: scaling within the 2–2000μm body size. *Limnol. Oceangr.*, **42**, 682–704.

Hickey, B. M. (1979) The California Current System—hypotheses and facts. *Prog. Oceanogr.*, **8**, 191–279.

Jacquet, S., Domaizon, I., Personnic, S. *et al.* (2005) Estimates of protozoan- and viral-mediated mortality of bacterioplankton in Lake Bourget (France). *Freshwater Biol.*, **50**, 627–645.

Jacquet, S., Hedal, M., Iglesias-Rodriguez, D. *et al.* (2002) Flow cytometric analysis of an *Emiliania huxleyi* bloom terminated by viral infection. *Aquat. Microb. Ecol.*, **27**, 111–124.

Kimmance, S. A. and Brussaard, C. P. D. (2010) Estimation of viral-induced phytoplankton mortality using the modified dilution. In Wilhelm, S. W., Weinbauer, M. G. and Suttle, C. A. (eds), *Manual of Aquatic Viral Ecology*. ASLO, Waco, TX, pp. 65–73.

Kimmance, S. A., Wilson, W. H. and Archer, S. D. (2007) Modified dilution technique to estimate viral versus grazing mortality of phytoplankton: limitations associated with method sensitivity in natural waters. *Aquat. Microb. Ecol.*, **49**, 207–222.

Landry, M. R. and Calbet, A. (2004) Microzooplankton production in the oceans. *ICES J. Mar. Sci.*, **61**, 501–507.

Landry, M. R. and Hassett, R. P. (1982) Estimating the grazing impact of marine micro-zooplankton. *Mar. Biol.*, **67**, 283–288.

Landry, M. R., Kirshtein, J. and Constantinou, J. (1995) A refined dilution technique for measuring the community grazing impact of microzooplankton, with experimental tests in the central equatorial Pacific. *Mar. Ecol. Prog. Ser.*, **120**, 53–63.

Landry, M. R., Ohman, M. D., Goericke, R. *et al.* (2009) Lagrangian studies of phytoplankton growth and grazing relationships in a coastal upwelling ecosystem off Southern California. *Prog. Oceanogr.*, **83**, 208–216.

Landry, M. R., Ohman, M. D., Goericke, R. *et al.* (2012) Pelagic community responses to a deep-water front in the California Current Ecosystem: overview of the A-Front study. *J. Plankton Res.*, **34**, 739–748.

Landry, M. R., Selph, K. E., Taylor, A. G. *et al.* (2011) Phytoplankton growth, grazing and production balances in the HNLC equatorial Pacific. *Deep-Sea Res. II*, **58**, 524–535.

Lynn, R. J. and Simpson, J. J. (1987) The California Current System: the seasonal variability of its physical characteristics. *J. Geophys. Res.*, **92**, 12947–12966.

Malfatti, F. and Azam, F. (2009) Atomic force microscopy reveals microscale networks and possible symbioses among pelagic marine bacteria. *Aquat. Microb. Ecol.*, **58**, 1–14.

Mann, K. H. and Lazier, J. R. N. (2006) *Dynamics of Marine Ecosystems: Biological–Physical Interactions in the Oceans*, 3rd edn. Blackwell Publishing, MA, pp. 216–253.

Massana, R., Del Campo, J., Dinter, C. *et al.* (2007) Crash of a population of the marine heterotrophic flagellate *Cafeteria roenbergensis* by viral infection. *Environ. Microbiol.*, **9**, 2660–2669.

Menden-Deuer, S. and Lessard, E. J. (2000) Carbon to volume relationships for dinoflagellates, diatoms, and other protist plankton. *Limnol. Oceanogr.*, **45**, 569–579.

Middelboe, M. (2000) Microbial growth rate and marine virus-host dynamics. *Microb. Ecol.*, **40**, 114–124.

Miki, T. and Jacquet, S. (2008) Complex interactions in the microbial world: unexplored key links between viruses, bacteria and protozoan grazers in aquatic environments. *Aquat. Microb. Ecol.*, **51**, 195–208.

Modigh, M. and Franzè, G. (2009) Changes in phytoplankton and microzooplankton populations during grazing experiments at a Mediterranean coastal site. *J. Plankton Res.*, **31**, 853–864.

Monger, B. C. and Landry, M. R. (1993) Flow cytometric analysis of marine bacteria with Hoechst 33342. *Appl. Environ. Microbiol.*, **59**, 905–911.

Monger, B. C., Landry, M. R. and Brown, S. L. (1999) Feeding selection of heterotrophic marine nanoflagellates based on the surface hydrophobicity of their picoplankton prey. *Limnol. Oceanogr.*, **44**, 1917–1927.

Nobel, R. T. and Fuhrman, J. A. (1998) Use of SYBR Green 1 for rapid epifluorescence counts of marine viruses and bacteria. *Aquat. Microb. Ecol.*, **14**, 113–118.

Patel, A., Nobel, R. T., Steel, J. A. *et al.* (2007) Viruses and prokaryote enumeration from planktonic aquatic environments by epifluorescence microscopy with SYBR Green 1. *Nat. Protoc.*, **2**, 269–276.

Pedros-Alio, C., Calderon-Paz, J. I. and Gasol, J. M. (2000) Comparative analysis shows that bacterivory, not viral lysis, controls the abundance of heterotrophic prokaryotic plankton. *FEMS Microbiol. Ecol.*, **32**, 157–165.

Pinheiro, M. D. O., Power, M. E., Butler, B. K. *et al.* (2007) Use of *Tetrahymena thermophile* to study the role of protozoa in inactivation of viruses in water. *Appl. Envrion. Microbiol.*, **73**, 643–649.

Pomeroy, L. R., Williams, P. J. leB., Azam, F. *et al.* (2007) The microbial loop. *Oceanography*, **20**, 28–33.

Poulin, F. J. and Franks, P. J. S. (2010) Size-structured planktonic ecosystems: constraints, controls and assembly instructions. *J. Plankton Res.*, **32**, 1121–1130.

Proctor, L. M. and Fuhrman, J. A. (1990) Viral mortality of marine-bacteria and cyanobacteria. *Nature*, **343**, 60–62.

Putt, M. and Stoecker, D. K. (1989) An experimentally determined carbon: volume ratio for marine "oligotrichous" ciliates from estuarine and coastal waters. *Limnol. Oceanogr.*, **34**, 1097–1103.

Samo, T. J., Pedler, B. E., Ball, G. I. *et al.* (2012) Microbial distribution and activity across a water mass frontal zone in the California Current Ecosystem. *J. Plankton Res.*, **34**, 802–814.

Shelford, E. J., Middelboe, M. J., Møller, E. F. *et al.* (2012) Virus-driven nitrogen cycling enhances phytoplankton growth. *Aquat. Microbiol. Ecol.*, **66**, 41–46.

Sherr, E. B. and Sherr, B. F. (1988) Role of microbes in pelagic food webs: a revised concept. *Limnol. Oceanogr.*, **35**, 1225–1227.

Sherr, E. B. and Sherr, B. F. (1993) Preservation and storage of samples for enumeration of heterotrophic protists. In Kemp, P., Sherr, E. B., Sherr, B. F. *et al.* (eds), *Handbook of Methods in Aquatic Microbial Ecology*. Lewis Publishers, Boca Raton, FL, pp. 207–212.

Sherr, E. B. and Sherr, B. F. (1994) Bacterivory and herbivory: key roles of phagotrophic protists in pelagic food webs. *Microb. Ecol.*, **28**, 223–235.

Sherr, E. B. and Sherr, B. F. (2000) Marine microbes: an overview. In Kirchman, D. L. (ed.), *Microbial Ecology of the Oceans*, 1st edn. Wiley, New York, pp. 13–46.

Sherr, B. F., Sherr, E. B. and McDaniel, J. (1992) Effect of protistan grazing on the frequency of dividing cells in bacterioplankton assemblages. *Appl. Environ. Microbiol.*, **58**, 2381–2385.

Šimek, K., Pernthaler, J., Weinbauer, M. G. *et al.* (2001) Changes in bacterial community composition and dynamics and viral mortality rates associated with enhanced flagellate grazing in a mesoeutrophic reservoir. *Appl. Environ. Microbiol.*, **67**, 2723–2733.

Smith, D. C., Simon, M., Alldredge, A. L. *et al.* (1992) Intense hydrolytic enzyme activity on marine aggregates and implications for rapid particle dissolutions. *Nature*, **359**, 139–142.

Strickland, J. D. H. and Parsons, T. R. (1972) *A Practical Handbook of Seawater Analysis*, 2nd edn, Bulletin 167. Fisheries Research Board of Canada, Ottawa.

Strom, S. L., Brahamsha, B., Fredrickson, K. A. *et al.* (2012) A giant cell surface protein in *Synechococcus* WH8102 inhibits feeding by a dinoflagellate predator. *Environ. Microbiol.*, **14**, 807–816.

Strom, S., Wolfe, G., Slajer, A. *et al.* (2003) Chemical defense in the microplankton. II. Inhibition of protist feeding by betadimethylsulfoniopropionate (DMSP). *Limnol. Oceanogr.*, **48**, 230–237.

Strub, P. T. and James, C. (2000) Altimeter-derived variability of surface velocities in the California current system: 2. Seasonal circulation and eddy statistics. *Deep-Sea Res. II*, **47**, 831–870.

Stukel, M. R., Landry, M. R., Benitez-Nelson, C. R. *et al.* (2011) Trophic cycling and carbon export relationships in the California Current Ecosystem. *Limnol. Oceanogr.*, **56**, 1866–1878.

Suttle, C. A. (1994) The significance of viruses to mortality in aquatic microbial communities. *Microb. Ecol.*, **28**, 237–243.

Suttle, C. A. (2000) Ecological, evolutionary, and geochemical consequences of viral infection of cyanobacteria and euaryotic algae. In Hurst, C. J. (ed.), *Viral Ecology*. Academic Press, San Diego, pp. 247–296.

Suttle, C. A. (2005) Viruses in the sea. *Nature*, **437**, 356–361.

Suttle, C. A. (2007) Marine viruses—major players in the global ecosystem. *Nat. Rev. Microbiol.*, **5**, 801–811.

Suttle, C. A. and Chan, A. M. (1993) Marine cyanophages infecting oceanic and coastal strains of *Synechococcus*: abundance, morphology, cross-infectivity and growth characteristics. *Mar. Ecol. Prog. Ser.*, **92**, 99–109.

Tai, V., Burton, R. S. and Palenik, B. (2011) Temporal and spatial distributions of marine *Synechococcus* in the Southern California Bight assessed by hybridization to bead-arrays. *Mar. Ecol. Prog. Ser.*, **426**, 133–147.

Taira, Y., Uchimiya, M. and Kudo, I. (2009) Simultaneous estimation of viral lysis and protozoan grazing on bacterial mortality using a modified virus-dilution method. *Mar. Ecol. Prog. Ser.*, **379**, 23–32.

Taniguchi, D. A. A., Landry, M. R., Franks, P. J. S. *et al.* (2014) Size-specific growth and grazing rates for picophytoplankton in coastal and oceanic regions of the eastern Pacific. *Mar. Ecol. Prog. Ser.*, **509**, 87–101.

Taylor, A. G., Goericke, R., Landry, M. R. *et al.* (2012) Sharp gradients in phytoplankton community structure across a frontal zone in the California Current Ecosystem. *J.* Plankton Res., **34**, 778–789.

Thingstad, T. F. (1998) A theoretical approach to structuring mechanisms in the pelagic food web. *Hydrobiologia*, **363**, 59–72.

Thingstad, T. F. (2000) Elements of theory for the mechanisms controlling abundance, diversity, and biogeochemical role of lytic bacterial viruses in aquatic systems. *Limnol. Oceanogr.*, **45**, 1320–1328.

Tsai, A. Y., Gong, G. C., Huang, J. K. *et al.* (2013a) Viral and nanoflagellate control of bacterial production in the East China Sea summer 2011. *Estuar. Coast. Shelf Sci.*, **120**, 33–41.

Tsai, A. Y., Gong, G. C. and Hung, J. K. (2013b) Seasonal variations of virus- and nanoflagellate-mediated mortality of heterotrophic bacteria in the coastal ecosystem of subtropical western Pacific. *Biogeoscience*, **10**, 3055–3065.

Ward, B. A., Dutkiewicz, S. and Follows, M. J. (2014) Modeling spatial and temporal patterns in size-structured marine plankton communities: top-down and bottom-up controls. *J. Plankton Res.*, **36**, 31–47.

Ward, B. A., Dutkiewicz, S., Jahn, O. *et al.* (2012) A size structured food-web model for the global ocean. *Limnol. Oceanogr.*, **57**, 1877–1891.

Waterbury, J. B. and Valois, F. W. (1993) Resistance to co-occurring phages enables marine *Synechococcus* communities to coexist with cyanophages abundant in seawater. *Appl. Environ. Microbiol.*, **1993**, 3393–3399.

Weinbauer, M. G. (2004) Ecology of prokaryotic viruses. *FEMS Microbiol. Rev.*, **28**, 127–181.

Weinbauer, M. G., Bonilla-Findji, O., Chan, A. M. *et al.* (2011) *Synechococcus* growth in the ocean may depend on the lysis of heterotrophic bacteria. *J. Plankton Res.*, **33**, 1465–1476.

Weinbauer, M. G., Hornák, K., Jezbera, J. *et al.* (2007) Synergistic and antagonistic effects of viral lysis and protistan grazing on bacteria biomass, production and diversity. *Environ. Microbiol.*, **9**, 777–788.

Weinbauer, M. G. and Peduzzi, P. (1995) Significance of viruses versus heterotrophic nanoflagellates for controlling bacterial abundance in the northern Adriatic Sea. *J. Plankton Res.*, **17**, 1851–1856.

Wilhelm, S. W. and Suttle, C. A. (1999) Viruses and nutrient cycles in the sea—viruses play critical roles in the structure and function of aquatic food webs. *Bioscience*, **49**, 781–788.

Zar, J. H. (1999) *Biostatistical Analysis*, 2nd ed. Prentice-Hall, Englewood Cliffs, NJ.

Zwirglmaier, K., Spence, E., Zubkov, M. V. *et al.* (2009) Differential grazing of two heterotrophic nanoflagellates on marine *Synechococcus* strains. *Environ. Microbiol.*, **11**, 1767–1776.